RARE METALS
Vol. 28, No. 6, Dec 2009, p. 612
DOI: 10.1007/s12598-009-0117-0

Synthesis of $LiFePO_4$ using $FeSO_4·7H_2O$ byproduct from TiO_2 production as raw material

PENG Zhongdong, CAO Yanbing, ZHOU Yulin, and HU Guorong

School of Metallurgical Science and Engineering, Central South University, Changsha 410083, China

Received 10 December 2008; received in revised form 16 March 2009; accepted 19 March 2009

Abstract

As the byproduct of TiO_2 industrial production, impure $FeSO_4·7H_2O$ was used for the synthesis of $LiFePO_4$. With the purified solution of $FeSO_4·7H_2O$, $FePO_4·xH_2O$ was prepared by a normal titration method and a controlled crystallization method, respectively. Then $LiFePO_4$ materials were synthesized by calcining the mixture of $FePO_4·xH_2O$, Li_2CO_3, and glucose at 700°C for 10 h in flowing Ar. The results indicate that the elimination of $FeSO_4·7H_2O$ impurities reached over 95%, and using $FePO_4·xH_2O$ prepared by the controlled crystallization method, the obtained $LiFePO_4$ material has fine and sphere-like particles. The material delivers a higher initial discharge specific capacity of 149 $mAh·g^{-1}$ at a current density of 0.1C rate (1C = 170 $mA·g^{-1}$); the discharge specific capacity also maintains above 120 $mAh·g^{1}$ after 100 cycles even at 2C rate. Thus, the employed processing is promising for easy control, low cost of raw material, and high electrochemical performance of the prepared material.

Keywords: lithium ion battery; cathode material; $LiFePO_4$; $FePO_4$; controlled crystallization

1. Introduction

Recently, olivine-structured $LiFePO_4$ reported by Goodenough's group [1] has attracted particular attention as the most promising candidate cathode material for lithium ion batteries. Comparing to commercialized $LiCoO_2$, $LiNiO_2$, $LiMn_2O_4$, and their derivatives, $LiFePO_4$ cathode material has outstanding advantages such as safety, low cost, and good environmental compatibility. However, due to the main disadvantages such as low electronic conductivity and low ion diffusivity, the rate performance of $LiFePO_4$ cathode material is still poor [2-8]. Several researchers reported that enhancement of electrochemical performance can be achieved by minimizing its particle size [9-12], doping supervalent metal ion [13-15], and effectively coating particles with carbon [16-21].

$LiFePO_4$ cathode material is usually prepared by conventional solid-state reaction of mechanically mixed lithium compounds, ferrous iron salts, and phosphates. Nowadays, little attention has been fixed on the ferric iron precursor of $LiFePO_4$ by proper low-cost production processing with the control of particle sizes and the modification of particle morphology to improve the electrochemical performance.

Now, about 50% production of global white titanium dioxide pigment is commercially manufactured by sulfate route. In addition, a large quantity of $FeSO_4·7H_2O$ byproduct is accompanied in the industrial production of sulfate route. While producing 1 t pigment, about 3-4 t $FeSO_4·7H_2O$ is produced. However, the utilization problem of $FeSO_4·7H_2O$ has not been solved yet, and resolving this problem has an important signification. In this paper, impure $FeSO_4·7H_2O$ was used as one of the starting materials to synthesize $LiFePO_4$. First, the impurities of $FeSO_4·7H_2O$ were eliminated, and then, pure $FeSO_4·7H_2O$ solution was obtained to prepare $FePO_4·xH_2O$ precursor. At last, $LiFePO_4$ cathode materials were prepared, adopting the obtained $FePO_4$. Contrasting with the two methods for the synthesis of $FePO_4$, an improved method to synthesize $LiFePO_4$ is introduced, and the results indicate that the employed processing has advantages such as easy control, low cost of raw material, and being suitable for industrial production.

2. Experimental

2.1. Purification of raw material $FeSO_4·7H_2O$

Byproduct FeSO4·$7H_2O$ from industrial TiO_2 production was used as raw material. However, with some impurities contained in this $FeSO_4·7H_2O$, purification was necessary. The main compositions of byproduct $FeSO_4·7H_2O$ were listed in Table 1. According to the data, the main impurities in the $FeSO_4·7H_2O$ were Mg, Mn, and Ti.

Corresponding author: PENG Zhongdong **E-mail:** pengzhd@263.net

Table 1. Analysis results of the main composition of raw material $FeSO_4·7H_2O$ wt.%

Al	As	Ba	Ca	Cd	Co	Cr	Cu	Mg
0.0020	0.0003	0.0001	0.0010	0.0002	0.0012	0.0003	0.0005	0.22
Mn	Mo	Ni	Pb	Si	**Ti**	V	Zn	Fe
0.20	0.0012	0.0002	0.0005	0.0010	0.30	0.0013	0.0096	19.3

The purification theory is as follows. At a lower pH condition, $Fe_3(PO_4)_2$ is a colloid compound deposition; it can absorb metal hydrated ions in solution, especially the hydrated ions that are high valent such as Mg^{2+}, Mn^{2+}, and Ti^{4+}. Then, these metal hydroniums can be deposited with $Fe_3(PO_4)_2$ and can be removed by filtration.

The purification method is that at room temperature, $FeSO_4·7H_2O$ was dissolved by deionized water with agitation, and H_3PO_4 was quantitatively added to transform some of Fe^{2+} to $Fe_3(PO_4)_2$ deposition. After complete reaction, the $Fe_3(PO_4)_2$ deposition was removed by filtration, and then, the purified $FeSO_4·7H_2O$ solution was gained to synthesize $FePO_4$.

2.2. Synthesis of $LiFePO_4$

First, the precursor $FePO_4·xH_2O$ powder was synthesized by the following methods, using purified $FeSO_4·7H_2O$ solution, H_3PO_4, H_2O_2, and $NH_3·H_2O$ as raw materials, according to the reaction:

$$FeSO_4·7H_2O + 2H_3PO_4 + 3H_2O_2 + 5NH_3·H_2O + xH_2O = FePO_4·xH_2O + (NH_4)_3PO_4 + (NH_4)_2SO_4 + 18H_2O.$$

Method 1: Normal titration method. Quantificational H_2O_2 was added into purified $FeSO_4·7H_2O$ solution with agitation to oxidize Fe^{2+}; and then, H_3PO_4 was added. When the reaction completed, quantificational 5% ammonia was added to adjust the pH. At last, the precipitation was filtrated, washed, and dried. Thus, the obtained $FePO_4·xH_2O$ powder was marked as precursor NM. Then, the $LiFePO_4$ material was synthesized by calcining the mixture of $FePO_4·xH_2O$, Li_2CO_3 and glucose at 700°C for 10 h in flowing Ar_2 and marked as $LiFePO_4$ S_1.

Method 2: The controlled crystallization method. The quantificational H_2O_2 was added into purified $FeSO_4·7H_2O$ solution to oxidize Fe^{2+}, and the prepared Fe^{3+} solution was pumped continuously into the reactor. Meanwhile, the H_3PO_4 solution was pumped into the same reactor under agitation, and 5% ammonia water was added to adjust the pH. The course of the reaction was carefully controlled. At last, the precipitation was filtrated, washed, and dried. As a result, $FePO_4·xH_2O$ powder was obtained and marked as precursor CM. Then, the $LiFePO_4$ material was synthesized by calcining the mixtures of $FePO_4·xH_2O$, Li_2CO_3, appropriate amount of glucose, and graphite at 700°C for 10 h in flowing Ar_2, and marked as $LiFePO_4$ S_2.

2.3. Characteristics of $LiFePO_4$

Thermogravimetric analysis (TGA)/differential scanning calorimetry (DSC) was carried out on an SDTQ-600 simultaneous thermal analyzer (TA Instruments Corporation, USA). The obtained $FePO_4·xH_2O$ was heated from room temperature to 1000°C in air at a heating rate of 10°C/min. The structure of samples was determined by X-ray diffraction (XRD, D/max-r A type Cu $K_{\alpha 1}$, 40 kV, 300 mA, 10-70°, Japan). The microstructure of products was observed by scanning electron microscopy (SEM, JEOL JSM-6360LV).

The cathodes were assembled into laboratory scale 2025 coin-type cells. The $LiFePO_4$ electrodes were prepared by slurring $LiFePO_4$ powder (80 wt.%), 10 wt.% acetylene black, and 10 wt.% polyvinylidene difluoride (PVDF) in *N*-methyl pyrrolidinone (NMP) and then formed by coating the slurry onto Al foils. After drying overnight at 393 K in a vacuum, the cells were assembled with the as-prepared cathode, lithium metal, and Celgard 2400 film in an ultrapure argon-filled glove box. The electrolytes were 1 mol/L $LiPF_6$ in ethylene carbonate (EC) + dimethyl carbonate (DEC) (volume ratio is 1:1). The electrochemical measurements were performed using LAND CT2001A test system between 2.5 and 4.1 V.

An EG&G PAR potentiostat/galvanostat model 273A, operated by model 270 software EG&G, was adopted to scan the potential at 0.4 mV/s by using the powder microelectrode assembled in argon on a dry box as the working electrode, lithium metal foils as the counter electrode, and 1 mol/L LiPF6/EC + DEC (1:1 in volume) as the electrolyte solution. The potential window was from 2.4 to 4.2 V.

3. Results and discussion

The main purpose of purification is to remove the impurities such as Mg, Mn, and Ti. The results are listed in Table 2.

According to Table 2, it is concluded that the more the quantity of H_3PO_4 is added, the higher the rate of purification is. However, the purification rate of adding 6 mL H_3PO_4 is only a little higher than that of 4 mL H_3PO_4. Considering that ion doping is an effective method to improve the electrochemical properties of $LiFePO_4$ [4, 13-15] and some minimum impurities (Mg, Mn, and Ti) remained are benefi-

cial for the performance of prepared $LiFePO_4$, thus, the ratio of $FeSO_4·7H_2O$ to H_3PO_4 was adopted as 28.0 g to 4 mL, simultaneously to reduce the loss of Fe, which was used to form $Fe_3(PO_4)_2$. Under this ratio, the main impurity in the obtained $FePO_4·xH_2O$ powders is Mg, which could improve the electrochemical performance of $LiFePO_4$.

Table 2. Purification results of raw material $FeSO_4·7H_2O$

Weight of $FeSO_4·7H_2O$ / g	Volume of H_3PO_4 / mL	Element	Elementary content in $FeSO_4·7H_2O$ / g	Elementary content in $FePO_4$ / g	Rate of purification / %
28.0	2	Mg	0.0616	0.0070	88.7
		Mn	0.0560	0.0054	90.3
		Ti	0.0840	0.0054	93.6
28.0	4	Mg	0.0616	0.0034	94.5
		Mn	0.0560	0.0020	96.5
		Ti	0.0840	0.0018	97.9
28.0	6	Mg	0.0616	0.0026	95.7
		Mn	0.0560	0.0018	96.8
		Ti	0.0840	0.0016	98.1

Fig. 1 shows the TGA/DSC curves of obtained $FePO_4·xH_2O$ precursor CM. On the DSC curve near 190°C, there is a very strong endothermic peak, according to the sharp weight loss on the TGA curve, which is related to the quick dehydration of $FePO_4·xH_2O$. On the DSC curve near 736°C, there is an exothermic peak, which is related to the transformation of amorphous $FePO_4$ to crystallized $FePO_4$. On the TGA curve, during 150°C to 225°C, there is about 20.23% weight loss, and chemical test indicates that the precursor has 29.68 wt.% iron. From these data, it can be inferred that the precursor can be described as $FePO_4·2H_2O$.

Fig. 2(a) shows the XRD patterns of $LiFePO_4$ samples S_1 and S_2. It can be seen that the diffraction patterns of the samples conform to an orthorhombic system with the space group *Pnma*, indicating that the well-crystallized single olivine-type phase is obtained. Moreover, it is concluded that some minim impurities that remained lead to no impurity phase growth with no impact on the synthesis of pure $LiFePO_4$, because there are small amounts of impurity ions, and impurity ions are doped in the form of solid-solution. During the synthesis process, Fe and different impurity elements are homogeneously mixed at atomic level in the solution, resulting in uniform distribution of impurity ions in the precipitation. Consequently, after calcining, the pure lithium phospho-olivine structure is formed.

However, a (123) peak was observed in the diffraction patterns of $LiFePO_4$ S_2 corresponding to graphite with addition of graphite. Additionally, it can be observed that compared with $LiFePO_4$ sample S_1, the diffraction peak position

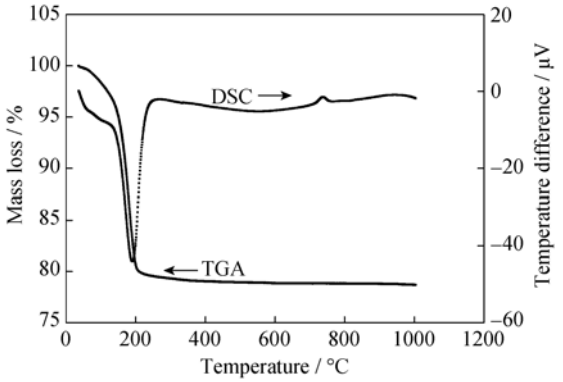

Fig. 1. TGA/DSC curves of the precursor CM.

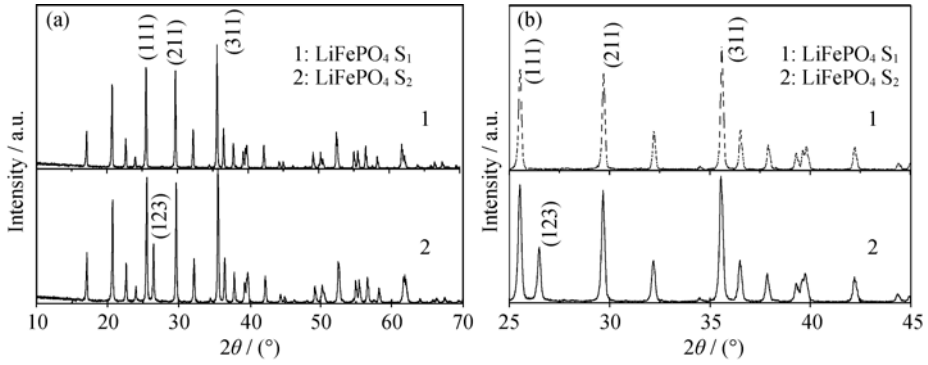

Fig. 2. XRD patterns of $LiFePO_4$ S_1 and $LiFePO_4$ S_2 (a) and the part magnification of (a) patterns (b).

of sample S_2 shifts to the left a little from the part magnification of Fig. 2(a) shown in Fig. 2(b), which indicates the increase of unit cell volume.

XRD data in Table 3 also reflects the same information. In addition, sample $LiFePO_4$ S_2 has the larger peak intensity ratio (I_{311}/I_{211}) of 1.2531, the lattice parameters are a = 1.0329 nm, b = 0.6011 nm, c = 0.4697 nm, and V = 0.2916 nm^3, which are larger than the corresponding parameters of sample $LiFePO_4$ S_1.

Fig. 3 shows SEM images of the precursor NM and precursor CM by two methods. The two precursor particles have an obvious difference in morphology. And the precursor NM has a structure of hexagonal sandwich particles, while precursor CM has a structure of agglomerated sphere-like particles, which is loose, and soft agglomeration formed during the crystallization process. By grinding, the agglomerate is destroyed and forms uniform spherical particles. Then, the precursor CM is advantageous to synthesize the regular and fine $LiFePO_4$ powders.

Fig. 4 shows the morphology of $LiFePO_4$ samples S_1 and S_2. According to SEM images, the shape of sample S_1 particles is irregular and agglomerated, with a wider range of particle size distribution. By contrast, the obtained sample S_2 particles develop well and exhibit spherical-like shape, with narrower particle size distribution. Furthermore, fine particle size and uniform distribution of S_2 crystallite are in favor of lithium ions diffusion and improving the charge-discharge performance.

Table 3. XRD data for various $LiFePO_4$ samples

Sample	Lattice parameters				I_{311}/I_{211}
	a / nm	b / nm	c / nm	V / nm^3	
$LiFePO_4$ S_1	1.0319	0.6001	0.469 1	0.2909	1.1215
$LiFePO_4$ S_2	1.0329	0.6011	0.469 7	0.2916	1.2531

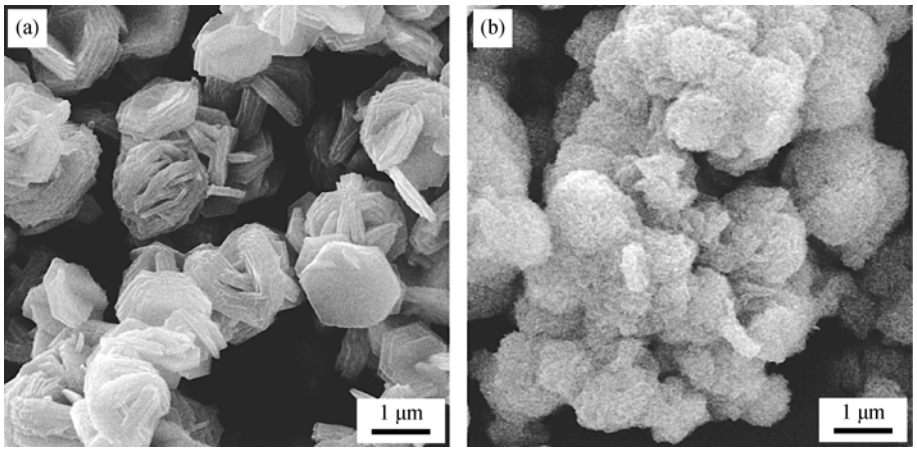

Fig. 3. SEM images of two precursors: (a) precursor NM; (b) precursor CM.

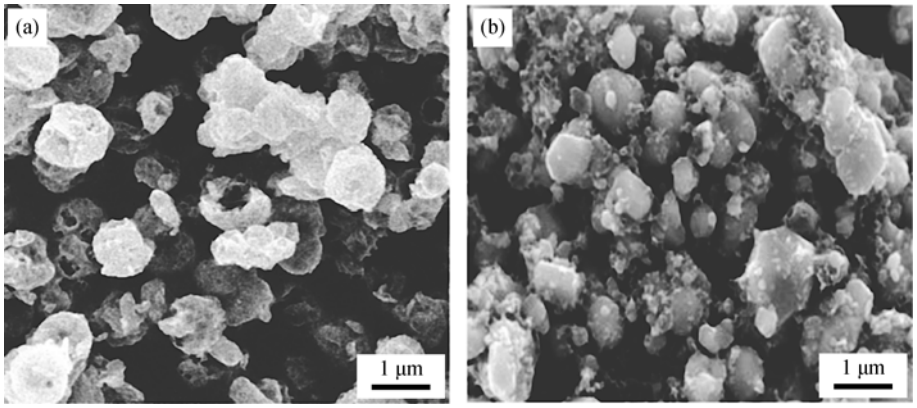

Fig. 4. SEM images of $LiFePO_4$ samples: (a) S_1; (b) S_2.

Fig. 5 shows the charge/discharge curves of $LiFePO_4$ samples S_1 and S_2 at different discharge rates. It shows that the electrochemical performance of samples S_2 synthesized by the controlled crystallization method is superior to that of sample S_1 by the normal titration method. It is displayed that sample S_1 has the initial specific capacity of 143 $mAh \cdot g^{-1}$, 111 $mAh \cdot g^{-1}$, and 104 $mAh \cdot g^{-1}$ at 0.1C, 1C, and 2C, respectively, while $LiFePO_4$ S_2 has 149 $mAh \cdot g^{-1}$, 133 $mAh \cdot g^{-1}$, and 127 $mAh \cdot g^{-1}$ correspondingly. It is obvious that sample S_2 has a higher specific capacity, and it exhibits more smooth discharge flat, which is closer to 3.4 V. The variation of discharge capacity with preparation methods can be explained in terms of particle size and microstructure homogeneity. The improved electrochemical performance of S_2 material originates from the uniform distribution of fine particles and homogeneous morphology by the controlled crystallization method. It is well known that the size and distribution of particles is critical in improving reversible lithium capacity and cycle ability for low-conductivity polyanion compounds [3, 10], and thus, the electrochemical performance of $LiFePO_4$ cathode material is better in sample S_2 with uniform and smaller particles, additionally, where the particles are in contact with carbon.

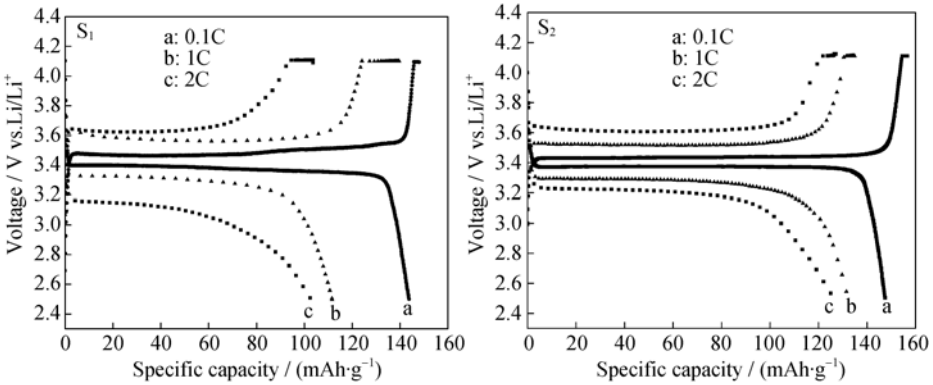

Fig. 5. Charge/discharge curves of $LiFePO_4$ S_1 and S_2 at different discharge rates.

Fig. 6 shows the cycling capability of $LiFePO_4$ S_2 at 1C and 2C rates. It indicates that $LiFePO_4$ S_2 has a discharge specific capacity higher than 130 $mAh \cdot g^{-1}$ at 1C rate after 100 cycles, and the sample shows good cycle capability with higher than 120 $mAh \cdot g^{-1}$ after 100 cycles even at 2C rate. Consequently, $LiFePO_4$ S_2 delivers good cycling stability at high discharge rate. Good cycle performance is attributed to uniform and small particles with carbon connection and improved bulk conductivity through remained metal elements doping, which enhances the lithium ion diffusivity and increases the electronic conductivity of crystallized powder [3-4].

Fig. 7 shows the corresponding cyclic voltammetry curve of $LiFePO_4$ S_2. A pair of redox reaction peaks appear in the CV curve. The oxidation peak at 3.62 V indicates the Li-ion deintercalation reaction during the positive sweep, and the reduction peak at 3.15 V symbolizes the Li-ion intercalation from the material in the anodic sweep. The sharp oxidation and reduction peaks indicate good kinetics of lithium intercalation and deintercalation reactions for the olivine structure cathode materials.

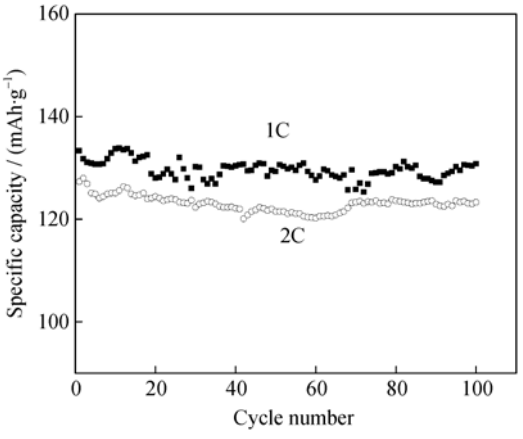

Fig. 6. Cycling performance of $LiFePO_4$ S_2 at 1C and 2C.

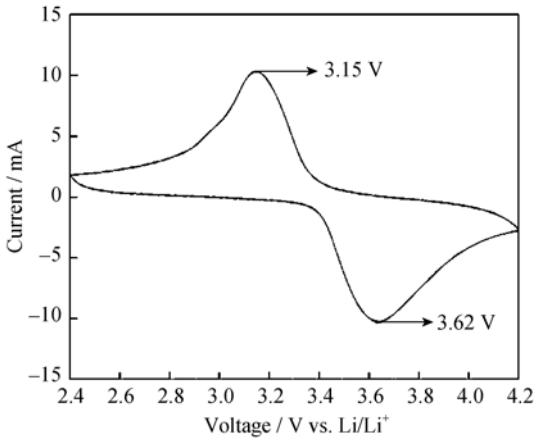

Fig. 7. CV curve of $LiFePO_4$ S_2 cathode material.

4. Conclusions

(1) Adding quantitative H_3PO_4 as the precipitator, the Mn and Ti impurities are well eliminated in the raw material $FeSO_4 \cdot 7H_2O$ byproduct from industrial TiO_2. The eliminative rates of Mn and Ti reach 96.5% and 97.9%, respectively. The remaining impurities are beneficial for the performance of the prepared material, with no impact on the synthesis of pure $LiFePO_4$.

(2) The spherical-like $FePO_4$ particles with a narrower size distribution are obtained by the controlled crystallization method, compared with those by normal titration method.

(3) Using precursor $FePO_4$ prepared by controlled crystallization processing, the obtained $LiFePO_4$ particles displays uniform size distribution and spherical-like shape. Furthermore, the $LiFePO_4$ S_2 sample has a higher specific capacity with the initial discharge specific capacity of 149 $mAh \cdot g^{-1}$at 0.1C, delivers the initial discharge specific capacity of 127 $mAh \cdot g^{-1}$ and maintains higher than 120 $mAh \cdot g^{-1}$ even after 100 cycles at 2C rate, showing good cyclability.

Acknowledgements

This work was financially supported by the National Key Technology R & D Program of China (No. 2007BAE12B01-1) and the National Natural Science Foundation of China (No. 50604018).

References

[1] Padhi A.K., Nanjundaswamy K.S., and Goodenough J.B., Phospho-olivines as positive-electrode materials for rechargeable lithium batteries, *J. Electrochem. Soc.*, 1997, **144** (4): 1188.

[2] Padhi A.K., Nanjundaswamy K.S., Masquelier C., and Goodenough J.B., Effect of structure on the Fe^{3+}/Fe^{2+} redox couple in iron phosphates, *J. Electrochem. Soc.*, 1997, **144** (5): 1609.

[3] Yamada A, Chung S.C., and Hinokuma K., Optimized $LiFePO_4$ for lithium battery cathodes, *J. Electrochem. Soc.*, 2001, **148** (3): A224.

[4] Chung S.Y., Bloking J.T., and Chiang Y.M., Electronically conductive phospho-olivines as lithium storage electrodes, *Nat. Mater.*, 2002, **1** (2): 123.

[5] Chen Z.H. and Dahn J.R., Reducing carbon in $LiFePO_4$/C composite electrodes to maximize specific energy, volumetric energy, and tap density, *J. Electrochem. Soc.*, 2002, **149** (9): A1184.

[6] Ravet N., Abouimrane A., Armand M., Chung S.Y., Bloking J.T., and Chiang Y.M., On the electronic conductivity of phospho-olivines as lithium storage electrodes, *Nat. Mater.* 2003, **2**: 702.

[7] Swoyer J.L, Barker J., and Saidi M.Y., Lithium iron(II) phospho-olivines prepared by a novel carbothermal reduction method, *Electrochem. Solid State Lett*., 2003, **6** (3): A53.

[8] Herle P.S., Ellis B., Coombs N., and Nazar L.F., Nano-network electronic conduction in iron and nickel olivine phosphates, *Nat. Mater.*, 2004, **3**: 147.

[9] Myung S.T., Komaba S., Hirosaki N., Yashiro H., and Kumagai N., Emulsion drying synthesis of olivine $LiFePO_4$/C composite and its electrochemical properties as lithium intercalation material, *Electrochim. Acta*, 2004, **49** (24): 4213.

[10] Park K.S., Kang K.T., Lee S.B., Kim G.Y., Park Y.J., and Kim H.G.., Synthesis of $LiFePO_4$ with fine particle by co-precipitation method , *Mater. Res. Bull.,* 2004, **39** (12): 1803.

[11] Cho T.H. and Chung H.T., Synthesis of olivine-type $LiFePO_4$ by emulsion-drying method, *J. Power Sources*, 2004, **133** (2): 272.

[12] Yang J.S. and Xu J.J., Nonaqueous sol-gel synthesis of high-performance $LiFePO_4$. *Electrochem. Solid State Lett*., 2004, **7** (12): A515.

[13] Wang G.X., Bewlay S., and Yao J., Characterization of $LiM_xFe_{1-x}PO_4$ (M = Mg, Zr, Ti) cathode materials prepared by the sol-gel method, *Electrochem. Solid State Lett*., 2004, **7** (12): A503.

[14] Hong J., Wang C.S., and Kasavajjula U., Kinetic behavior of $LiFeMgPO_4$ cathode material for Li-ion batteries, *J. Power Sources*, 2006, **162** (2): 1289.

[15] Hu G.R., Gao X.G., Peng Z.D., Du K., Tan X.Y., and Liu Y.J., Influence of Ti^{4+} doping on electrochemical properties of LiFePO4/C cathode material for lithium-ion batteries, *Trans. Nonferrous Met. Soc. Chin.* **2007, 17** (2): 296.

[16] Belharouak I., Johnson C., and Amine.K., Synthesis and electrochemical analysis of vapor-deposited carbon-coated $LiFePO_4$, *Electrochem. Commun.,* 2005, **7** (10): 983.

[17] Shin H.C., Cho W., and Jang H., Electrochemical properties of carbon-coated $LiFePO_4$ cathode using graphite, carbon black, and acetylene black, *Electrochim. Acta*, 2006, **52** (4): 1472.

[18] Peng Z.D., Gao X.G., Hu G.R., Tan X.Y., DuK., Deng X.R., and Liu Y.X., Technological optimization of $LiFePO_4$ preparation by water quenching treatment, *J. Cent. South Univ. Technol.*, 2007, **14** (5): 56

[19] Wang L.N., Zhang Z.G., and Zhang K.L., A simple, cheap soft synthesis routine for $LiFePO_4$ using iron(III) raw material, *J. Power Sources*, 2007, **167** (1): 200.

[20] Liu H., Xie J.Y., and Wang K., Synthesis and characterization of $LiFePO_4/(C + Fe_2P)$ composite cathodes, *Solid State Ionics*, 2008, **179** (27-32): 1768.

[21] Kuwahara A., Suzuki S., and Miyayama M., High-rate properties of $LiFePO_4$/carbon composites as cathode materials for lithium-ion batteries, *Ceram. Int*., 2008, **34** (4): 863.